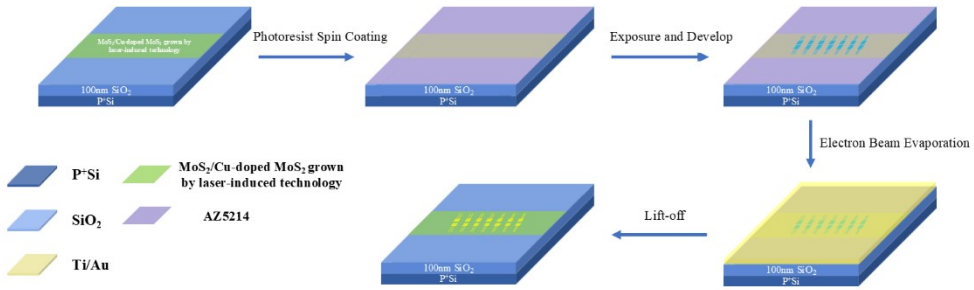

Figure S1. The process flow chart of MoS_2/Cu-doped MoS_2 FETs

The device fabrication process is shown in Figure S1. The electrode patterns for the laser-synthesized thin films were fabricated using photolithography, which includes the steps of spin-coating the photoresist, exposure, and development. The electrodes were then deposited using electron beam evaporation (EBE). Finally, the photoresist was removed to complete the fabrication of the FET device.

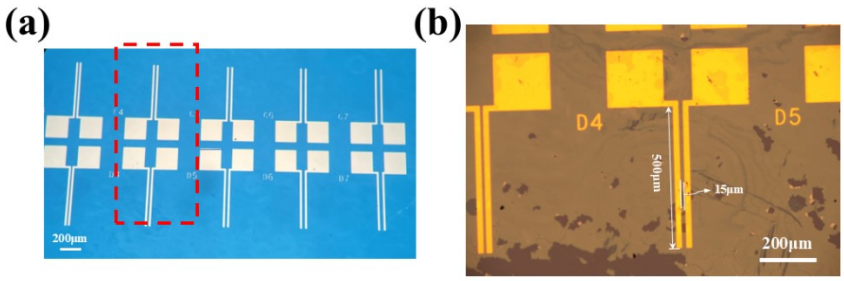

Figure S2. (a) Optical microscopy image of the fabricated FET, (b) optical microscopy image of the fabricated electrodes

The optical microscopy image of the fabricated devices is shown in Figure S2. We selected the C_4/D_4 electrode pair for I-V testing, with specific dimensions of W = 15 μm and L = 500 μm.

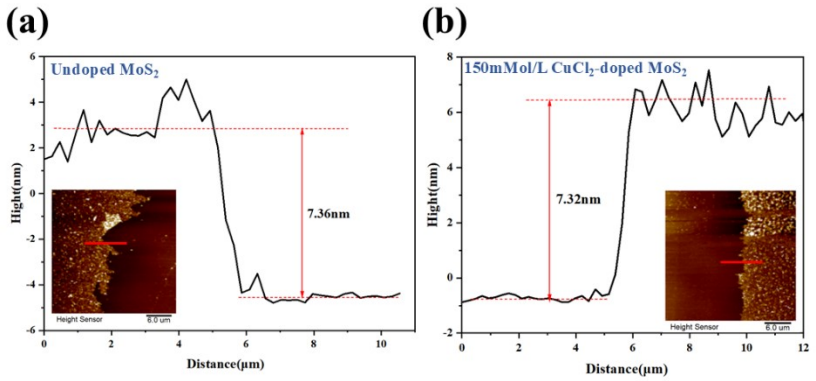

Figure S3. AFM characterization of film thickness:(a) thickness of undoped MoS_2 film, (b)thickness of 150 mMol/L $CuCl_2$-doped MoS_2 film

AFM measurements were conducted to provide thickness information for the films, as shown in Figure S3. Both undoped MoS_2 and Cu-doped MoS_2 films were approximately 7 nm thick. The MoS_2 films synthesized via pulsed laser technology were multilayered(~11-layer).

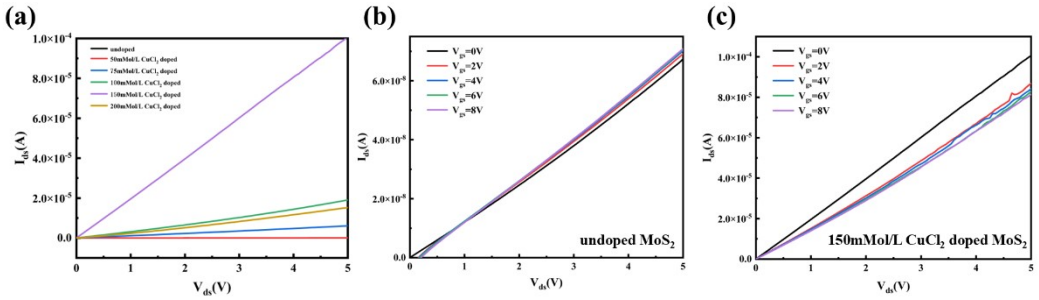

Figure S4. (a) Output characteristic curves at V_{gs}=0V for different $CuCl_2$ doping concentrations, (b) output characteristic curve of undoped MoS_2 FET, (c) output characteristic curve of 150 mMol/L $CuCl_2$-doped MoS_2 FET

The output characteristic curves of undoped MoS_2 FETs and Cu-doped MoS_2 FETs is shown in Figure S4. Figure S4(a) has plotted the output curves of MoS_2 FETs with different Cu doping concentrations at V_{gs}=0V. It can be observed that with 150 mMol/L $CuCl_2$ doping, the current increases by at least two orders of magnitude, indicating an enhancement in the film's electrical conductivity.